THE JOURNAL OF BIOLOGICAL CHEMISTRY VOL. 283, NO. 30, pp. 21002–21010, July 25, 2008

In Vivo Targeted Deletion of Calpain Small Subunit, *Capn4*, in Cells of the Osteoblast Lineage Impairs Cell Proliferation, Differentiation, and Bone Formation*

Received for publication, December 19, 2007, and in revised form, May 29, 2008 Published, JBC Papers in Press, May 30, 2008, DOI 10.1074/jbc.M710354200

Masako Shimada[‡1], **Peter A. Greer**[§], **Andrew P. McMahon**[¶], **Mary L. Bouxsein**[‖], **and Ernestina Schipani**[‡]

From the [‡]*Endocrine Unit, Massachusetts General Hospital and Department of Medicine, Harvard Medical School, Boston, Massachusetts, 02114, the* [§]*Queen's University Cancer Research Institute, Kingston, Ontario, Canada K7L 3N6, the* [¶]*Department of Molecular and Cellular Biology, Harvard University, Cambridge, Massachusetts 02138, and the* [‖]*Orthopedic Biomechanics Laboratory, Beth Israel Deaconess Medical Center, Boston, Massachusetts, 02215*

Calpains are intracellular cysteine proteases, which include widely expressed μ- and m-calpains (1). Both μ-calpains and m-calpains are heterodimers consisting of a large catalytic subunit and a small regulatory subunit. The calpain small subunit encoded by the gene *Capn4* directly binds to the intracellular C-terminal tail (C-tail) of the receptor for parathyroid hormone and parathyroid hormone-related peptide and modulates its cellular functions in osteoblasts *in vitro* (2). To investigate a potential role of the calpain small subunit in osteoblasts *in vivo*, we generated osteoblast-specific *Capn4* knock-out mice using the *Cre*-LoxP system (3). Mutant mice had smaller bodies with shorter limbs, reduced trabecular bone with thinner cortices, and decreased osteoblast number. *In vitro* analysis confirmed that deletion of *Capn4* in osteoblasts severely affected multiple osteoblast functions including proliferation, differentiation, and matrix mineralization. Collectively, our findings provide the first *in vivo* demonstration that the calpain small subunit is essential for proper osteoblast activity and bone remodeling.

Calpains are a family of Ca^{2+}-dependent intracellular cysteine proteases that include ubiquitously expressed μ- and m-calpains (1, 4). Both μ-calpains and m-calpains form heterodimers consisting of a large catalytic subunit (80 kDa) encoded by the genes *Capn1* and *Capn2*, respectively, and a small regulatory subunit (28 kDa) encoded by the gene *Capn4* (1). Disruption of *Capn4* eliminates both μ-calpains and m-calpain activities in embryonic fibroblasts (5), suggesting that the calpain small subunit is essential for maintenance of calpain stability and activity. Notably, genetic ablation of *Capn4* results in early embryonic lethality, which demonstrates an essential role of the calpain small subunit during development (5, 6).

Several lines of evidence suggest that calpains are necessary for proper osteoblast function *in vitro* (7–11). However, a physiological role of calpains in osteoblasts *in vivo* remains to be established. Chemical inhibition of calpain activity reduces osteoblast proliferation and differentiation in the MC3T3-E1 osteoblastic cell line (11). Moreover, we have previously reported that the calpain small subunit directly binds to the intracellular C-tail of the receptor for PTH[2] and PTH-related peptide and modulates its ligand-mediated cellular functions (2). Both ligands are known regulators of bone homeostasis *in vivo* through their direct actions on cells of the osteoblast lineage (12–14). Taken together, these findings suggest that the calpain small subunit could play a critical but yet unknown role in osteoblast biology *in vivo*.

To test this hypothesis, we have conditionally ablated *Capn4* in cells of the osteoblast lineage *in vivo* by using the *Cre*-LoxP system. Lack of the calpain small subunit in osteoblasts caused a significant decrease of both trabecular and cortical bone, which was associated with a severe impairment of osteoblast proliferation and differentiation. These findings are the first *in vivo* evidence that the calpain small subunit plays a crucial role in osteoblast function and bone homeostasis.

EXPERIMENTAL PROCEDURES

Generation of Osx-Cre$^{+/-}$ Capn4$^{flox/flox}$ Mice—Mice homozygous for floxed *Capn4* alleles (*Capn4$^{flox/flox}$*) were crossed with those expressing *Cre* under the control of osterix promoter (Osx-*Cre$^{+/-}$*) to generate Osx-*Cre$^{+/-}$Capn4$^{flox/+}$* mice (15–17). These mice were then crossed with either *Capn4$^{flox/flox}$* or *Capn4$^{flox/+}$* mice to generate Osx-*Cre$^{+/-}$Capn4$^{flox/flox}$* mutant mice. All experiments were performed in compliance with the guiding principles of the Guide for the Care and Use of Laboratory Animals and approved by the subcommittee on Research Animal Care of the Massachusetts General Hospital (MGH).

Genotype Analysis—Genomic DNA was isolated from tail biopsies as described previously (18). PCR-based strategies were used to genotype these mice. The *Cre* transgene was detected by PCR using the primers P1 (5′-CGCGGTCTGGCAGTAAAAACTATC-3′) and P2 (5′-CCCACCGTCAGTACGTGAGAT ATC-3′) to generate an internal sequence of *Cre*. Taking an advantage of a floxed construct, in which an intron 9 was shortened by 1.6 kilobase pairs (kbp), the *Capn4* floxed and wild-type alleles were determined using two sets of

* This work was supported, in whole or in part, by National Institutes of Health Grant R01 DK072102 (to M. S.). This work was also supported by Canadian Institutes of Health Research Grant MOP-81189 (to P. A. G.). The costs of publication of this article were defrayed in part by the payment of page charges. This article must therefore be hereby marked "*advertisement*" in accordance with 18 U.S.C. Section 1734 solely to indicate this fact.

[1] To whom correspondence should be addressed. Tel.: 617-726-3966; Fax: 617-726-1703; E-mail: shimada@helix.mgh.harvard.edu.

[2] The abbreviations used are: PTH, parathyroid hormone; μCT, microcomputed tomography; BrdUrd, bromodeoxyuridine; αMEM, α-minimum essential medium; ALP, alkaline phosphatase; qPCR, quantitative PCR; siRNA, small interfering RNA; UMR, UMR106-01; kbp, kilobase pairs.

PCR reactions (15, 19). The floxed and wild-type alleles were determined as 0-bp (no amplified product) and 1.0-kbp PCR products, respectively, using primers P3 (5′-GTCAGGCTAGATGCCATGTTCC-3′) in exon 9 and P4 (5′-CGACTATCCGAGCGCTGCC-3′) within a sequence deleted in floxed allele in intron 9 and as 0.4-kbp and 2.0-kbp PCR products, respectively, using primers P3 (5′-GTC AGGCTAGATGCCATGTTCC-3′) and P5 (5′-GTTCACTTGGATCTGTCCGGTGCC-3′) corresponding to sequences in exons E9 and E10.

Serology—Ionized calcium was measured with the Ciba-Corning 634 Ca^{2+}/pH analyzer (Ciba-Corning Diagnostics Corp., Medfield, MA). Serum levels of osteocalcin (Biomedical Technologies Inc., Stoughton, MA) and tartrate-resistant acid phosphatase (TRACP) 5b (Immunodiagnostic Systems, Tyne and Wear, UK) were determined using enzyme-linked immunosorbent assays as described by the manufacturers' instructions.

Whole Mount Skeletal Staining—The whole mount skeletal staining was performed as described previously (20). Briefly, newborn mice were fixed in ethanol for 5 days and then in acetone for 2 days. Staining with Alizarin red S and Alcian blue was performed for 3 days at 37 °C. After washing with distilled water, the skeleton was cleared in 1% KOH and taken through graded steps into 100% glycerol.

Sample Preparation and Histological Analysis—For histological analysis, Osx-$Cre^{+/-}Capn4^{flox/flox}$ and sex-matched control littermates (Osx-$Cre^{+/-}Capn4^{flox/+}$ and $Capn4^{flox/flox}$) were sacrificed at birth and at 2, 4, 9, and 12 weeks of age. Tissues from Osx-$Cre^{+/-}Capn4^{flox/flox}$, and control littermates were fixed and stored as described previously (21). In selected cases, hind limbs were decalcified, and paraffin blocks were prepared by standard histological procedures. To detect osteoclast-like cells, tartrate-resistant acid phosphatase (TRAP) staining was performed using an acid phosphatase detection kit (Sigma-Aldrich) for some selected samples.

In Situ Hybridization—*In situ* hybridization analysis was performed as described previously (22). Complementary ^{35}S-labeled riboprobes were transcribed from the plasmids encoding mouse type I collagen (*Col.1*), mouse matrix metalloproteinase *(MMP)13*, mouse osteocalcin (*OC*), mouse osteopontin (*OP*), and rat *TRAP* using Riboprobe systems from Promega (Madison, WI).

Histomorphometry—For dynamic histomorphometry, animals were injected intraperitoneally with fluorochromes, calcein, and demeclocycline (20 μg/g of body weight, Sigma-Aldrich), 3 and 10 days before sacrifice, respectively. Bones were fixed and embedded in methyl methacrylate resin as described previously (21). Five-micrometer sections were stained with Masson Trichrome or coverslipped unstained, and histomorphometric analysis was performed with the Osteomeasure system (Osteometrics Inc., Atlanta, GA) using standard procedures. Tibial sections were measured in the proximal metaphysis beginning 340 μm below the chondro-osseous junction.

Microcomputed Tomography (μCT)—High resolution images of the femur and lumber vertebra were acquired by using a desktop microtomographic imaging system (MicroCT40: Scanco Medical, Basserdorf, Switzerland) as described previously (23–25). We assessed trabecular bone morphology in the distal femoral metaphysis and the fifth lumbar vertebral body and cortical bone morphology at the femoral mid-shaft (voxel size = 12 μm). For trabecular bone, we measured bone volume fraction (*BV/TV*, %), trabecular number (*Tb.N*, 1/mm), and trabecular separation (*Tb.Sp*, μm) (see Fig. 3). For cortical bone, we assess the total cross-sectional area (*TA*, mm^2), cortical bone area (*BA*, mm^2), cortical thickness (μm), and the polar moment of inertia (*MOIpolar*, mm^4) (see Fig. 3).

Analysis of Bromodeoxyuridine Incorporation—Two-week-old mice were injected intraperitoneally with 100 μg of bromodeoxyuridine (BrdUrd) and 12 μg of fluorodeoxyuridine per g of body weight 2 h before sacrifice (Sigma-Aldrich). After sacrifice, hind limbs were dissected, fixed, decalcified, and embedded in paraffin, and longitudinal sections across the tibia and femur were obtained. To identify actively proliferating cells, nuclei that had incorporated BrdUrd were detected using a Zymed BrdUrd immunostaining kit (Zymed Laboratories Inc., South San Francisco, CA). For each section, high power field images of the primary spongiosa and the proliferating chondrocyte layer were photographed. All BrdUrd-positive (black) and BrdUrd-negative (light blue) nuclei in these zones were counted separately. Four or five nonconsecutive sections were counted for each of two or three $Capn4^{flox/flox}$, Osx-$Cre^{+/-}Capn4^{flox/+}$, and Osx-$Cre^{+/-}Capn4^{flox/flox}$ littermate specimens at each time point.

Determination of Apoptotic Osteoblasts in Vivo—Apoptotic osteoblasts were detected in sections of decalcified tibias of 2-week-old $Capn4^{flox/flox}$, Osx-$Cre^{+/-}Capn4^{flox/+}$ mice, and Osx-$Cre^{+/-}Capn4^{flox/flox}$ littermates by a terminal deoxynucleotidyl transferase-mediated nick-end labeling reaction using reagents from the *in situ* cell death detection kit, POD (Roche Diagnostics). The sections were counterstained with 4,6-diamidino-2-phenylindole (Vector Laboratories, Burlingame, CA).

Osteoblast Isolation and Culture—Osteoblasts were isolated from calvariae of newborn mice by serial digestion in α-minimum essential medium (αMEM) (Invitrogen) containing 0.25 mg/ml type I and 0.75 mg/ml type II collagenases (Worthington, Lakewood, NJ). Calvariae were digested for 15 min at 37 °C with constant agitation. The digestion solution was collected, washed with fresh medium, and digested five additional times. Digestions 3–6 were collected, washed with αMEM, and cultured in αMEM supplemented with 10% fetal bovine serum (HyClone, Logan, UT), 1% penicillin/streptomycin (Invitrogen Corp.) for 48 h. Medium was changed every other day.

Adenovirus Infection—Monolayer $Capn4^{flox/flox}$ osteoblasts were infected with either control (adeno-*lacZ*) or *Cre*-recombinase adenovirus (adeno-*Cre*) at a multiplicity of infection of 100 for most experiments (26). Osteoblasts were harvested after 48 h. Genomic DNA and total RNA were extracted from osteoblasts for determination of efficiency of *Cre*-recombinase.

Alkaline Phosphatase (ALP) Activity—ALP activity was measured in cell layers using a *p*-nitrophenyl phosphate substrate (Sigma-Aldrich) as described previously (27). Cells were cultured in αMEM containing 10% fetal bovine serum, 1% penicillin/streptomycin for 7, 14, and 21 days, respectively.

Bone Nodule Assay—Cells were cultured in αMEM with 10% fetal bovine serum and 1% penicillin/streptomycin supplemented with 50 μg/ml L-ascorbic acid and 10 mM β-glycerophosphate (Sigma-Aldrich) (differentiation medium) for 21 and 28 days, respectively. Cells were then fixed with 70% ethanol, and mineralized calcium-phosphate deposits were stained with either Alizarin red S or von Kossa. Bone nodules were counted using a dissecting microscope. In some experiments, Alizarin red S dye was eluted and quantified as described elsewhere (27).

Real-time Quantitative PCR (qPCR)—The efficiency of *Cre*-recombinase driven by the osterix promoter or adeno-*Cre* was assessed using real-time qPCR on genomic DNA isolated from tibiae of Osx-$Cre^{+/-}Capn4^{flox/flox}$ and $Capn4^{flox/flox}$ mice and from primary osteoblasts harvested from $Capn4^{flox/flox}$ mice infected with either adeno-*lacZ* or adeno-*Cre*. In brief, tibial diaphyses of Osx-$Cre^{+/-}Capn4^{flox/flox}$ and $Capn4^{flox/flox}$ mice were isolated, extensively flushed in phosphate-buffered saline, and incubated in αMEM containing collagenases I and II at 37 °C for 45 min to remove hematopoietic cells and soft tissues. The diaphyses were then crushed and further digested with collagenase in αMEM medium. Genomic DNA was isolated using standard protocols. Real-time qPCR was then performed at 60 °C for 40 cycles in the Opticon continuous fluorescence detector by using a SYBR Green PCR kit (Qiagen) and primers P3 and P5. To determine RNA expression of various genes, total RNA was extracted from cells by using the RNeasy Mini kit (Qiagen). First-strand cDNA was synthesized using the First Strand cDNA synthesis kit for reverse transcription-PCR (Roche Diagnostics) followed by real-time qPCR. Samples were run in duplicate, and the results were normalized to *GAPDH* expression (26). Primer sequences were as follows: *ALP*, P6 (5′-CACGCGATGCAACACCACTCAGG-3′) and P7 (5′-GCATGTCCCCGGGCTCAAAGA-3′); *Capn4*, P8 (5′-CCAGCTGGCTGGAGACGAC-3′) and P9 (5′-GCGGCCTCAAAGGCGCCTG-3′); *Col.1*, P10 (5′-CACCCTCAAGAGCCTG AGTC-3′) and P11 (5′-GTTCGGGCTGATGTACCAGT-3′); *GAPDH*, P12 (5′-AACTACATGGTCTACATGTTCCA-3′) and P13 (5′-CCATTCTCGGCCTTGACTGT-3′); *NaPi3*, P14 (5′-CACCCATATGGCTTCTGCTT-3′) and P15 (5′-CAGGAATTCATAGCCCAGGA-3); *OC*, P16 (5′-ACCCTGGCTGCGCTCTGTCTCT-3′) and P17 (5′-GATGCGTTTGTAGGCGGTCTTCA-3′); *OP*, P18 (5′-CTCCTTGCGCCACAGAATG-3′) and P19 (5′-TGGGCAACAGGGATGACA-3′); *PGK*, P20 (5′-GGAACGGGTCGTGATGA-3′) and P21 (5′-GC CTTGATCCTTTGGTTGTTTT-3′); *Runx2*, P22 (5′-AGCTACGAAATGCCTCTGCTG-3′) and P23 (5′-GATCGTTGAACCTGGCCACT-3′); and c-*fos* P24 (5′-CCACGGTGACAGCCATCTCCACCA-3′) and P25 (5′-GGCTGCAGCCATCTTATTCCTTTCCC-3′) (19, 28–30).

Osteoblast Apoptosis Assay in Vitro—Forty-eight h after adenoviral infection, osteoblasts were replated in 24-well plates at a density of 2.5×10^4 cells/cm^2. Cells were stained with annexin V-PE and 7-aminoactinomycin D using Guava PCA Nexin kit and analyzed by Guava personal cytometer (Guava Technology Inc., Hayward, CA).

Gene Silencing by siRNA—UMR106-01 (UMR) rat osteosarcoma cells were plated at a density of 5×10^4 cells/cm^2 in 24-well plates. *Capn4* and control nonfunctional siRNA were transfected into UMR cells using Oligofectamine as recommended by the manufacture (Invitrogen). Cells were harvested 48 h after transfection.

Commercially available *Capn4* siRNA sequences are as follows: siRNA/*Capn4*-1, P26/P27 (5′-ACUGACCGACAGACCAUUGGUA-3′ and 5′-UACCAAUGGUCGAUCGGUCAGU-3′); siRNA/*Capn4*-2, P28/P29 (5′-GGAUCCGACUCUGCUGCAAACAUGU-3′ and 5′-ACAUGUUUGCAGCAGAGUCGGUC-3′) (Invitrogen). Efficiency of *Capn4* siRNA was assessed by calpain activity as described previously (2).

Statistics—Data were calculated from 3 to 5 independent experiments and expressed as the mean ± S.E. of either duplicate or triplicate determinations. Statistical analysis was performed using the analysis of variance or the unpaired Student's *t* test. Statistical significance was determined using Fisher's projected least significant difference, and p values less than 0.05 were accepted as significant.

RESULTS

Generation of Mice Lacking Capn4 in Cells of the Osteoblast Lineage and Characterization of Their Gross Phenotype—Mice expressing *Cre* under the control of the osterix promoter (Osx-$Cre^{+/-}$) were crossed with floxed *Capn4* mice ($Capn4^{flox/flox}$) to produce Osx-$Cre^{+/-}Capn4^{flox/+}$ mice, which were then mated with either $Capn4^{flox/flox}$ or $Capn4^{flox/+}$ to generate osteoblast-specific *Capn4* knock-out mice, Osx-$Cre^{+/-}Capn4^{flox/flox}$. Osx-$Cre^{+/-}Capn4^{flox/+}$, Osx-$Cre^{+/-}Capn4^{+/+}$ and $Capn4^{flox/flox}$ were also used in the study as control littermates. Efficiency of *Cre* activity assessed by real-time qPCR of either genomic DNA or RNA isolated from 4-week-old mutant tibiae was ~85% (genomic DNA, 86.5 ± 2.5%; RNA, 88.7 ± 0.8%).

Osx-$Cre^{+/-}Capn4^{flox/flox}$ (mutant) mice were born at the expected Mendelian frequency and were viable into adulthood and fertile. Their mean body weight in both sexes was reduced starting from 4–5 weeks of age in comparison with Osx-$Cre^{+/-}Capn4^{flox/+}$, $Capn4^{flox/flox}$, and Osx-$Cre^{+/-}Capn4^{+/+}$ control littermates. Surprisingly, at 10 weeks of age, body weight of Osx-$Cre^{+/-}Capn4^{flox/+}$ male mice was also significantly lower than that of the other controls, $Capn4^{flox/flox}$ and Osx-$Cre^{+/-}Capn4^{+/+}$ (Fig. 1*C*). Ionized calcium levels of 8-week-old mice were similar between mutant and control littermates.

The newborn skeleton of Osx-$Cre^{+/-}Capn4^{flox/flox}$ mice was definitively smaller than that of $Capn4^{flox/flox}$ and Osx-$Cre^{+/-}Capn4^{flox/+}$ littermates but did not exhibit any obvious patterning defect (Fig. 1*A*). Notably, mineralization of the skull was strikingly impaired in Osx-$Cre^{+/-}Capn4^{flox/flox}$ mice (Fig. 1*B*).

Osx-$Cre^{+/-}Capn4^{flox/flox}$ Mice Have Decreased Trabecular Bone and Reduced Expression of Osteoblast-specific Markers—Detailed histological and *in situ* hybridization analyses were then performed on hind limbs isolated from 2-, 4-, and 9-week-old male mice, respectively, to investigate a putative role of *Capn4* in bone modeling and remodeling. Tibiae of 2-week-old Osx-$Cre^{+/-}$ $Capn4^{flox/flox}$ mice had markedly reduced trabecular bone when compared with both Osx-$Cre^{+/-}Capn4^{flox/+}$ and $Capn4^{flox/flox}$ control littermates (Fig. 2*A*). Moreover, expression of osteoblast markers such as *MMP13*, *Col.1*, and *OC* was severely impaired in mutant bones (Fig. 2*A* and data not

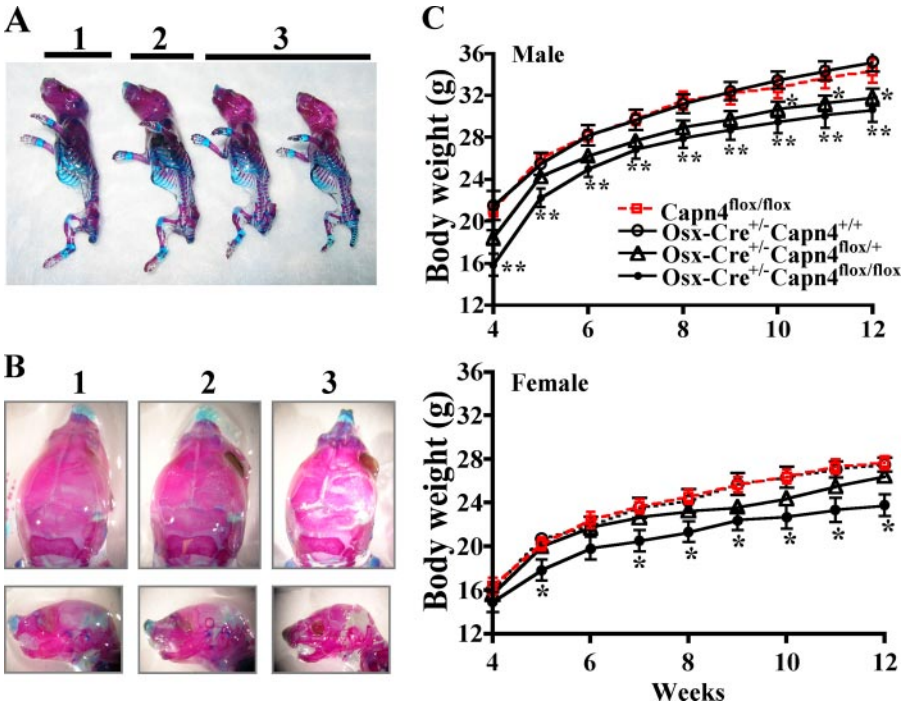

FIGURE 1. **Lack of *Capn4* in cells of the osteoblast lineage causes delay in skeletal development.** *A* and *B*, whole mount skeletal staining with Alizarin red S and Alcian blue. The newborn skeleton of Osx-$Cre^{+/-}$ $Capn4^{flox/flox}$ mice was smaller with no obvious patterning defects (*A*) but exhibited impaired mineralization of the skull (*B*) when compared with the controls. *1*, *2*, and *3* indicate $Capn4^{flox/flox}$, Osx-$Cre^{+/-}Capn4^{flox/+}$, and Osx-$Cre^{+/-}Capn4^{flox/flox}$, respectively. *C*, the mean body weight of Osx-$Cre^{+/-}Capn4^{flox/flox}$ mice was significantly reduced in both males and females when compared with $Capn4^{flox/flox}$, Osx-$Cre^{+/-}Capn4^{flox/+}$, and Osx-$Cre^{+/-}Capn4^{+/+}$ littermates. $Capn4^{flox/flox}$ (10 males; 10 females), Osx-$Cre^{+/-}Capn4^{+/+}$ (10 males; 6 females), Osx-$Cre^{+/-}Capn4^{flox/+}$ (15 males; 11 females), and Osx-$Cre^{+/-}Capn4^{flox/flox}$ (10 males; 6 females) were weighed weekly from 4 to 12 weeks. *, $p < 0.05$ and **, $p < 0.001$.

shown). A similar phenotype was also detectable in 4- and 9-week-old mutant mice of either sex (Fig. 2, *B* and *C*, and data not shown). Surprisingly, at these ages, Osx-$Cre^{+/-}$ $Capn4^{flox/flox/+}$ mice displayed a loss of trabecular bone, which was virtually indistinguishable from that of Osx-$Cre^{+/-}$ $Capn4^{flox/flox}$ mutants, as shown by routine histology and detection of *Col.1* mRNA by *in situ* hybridization analysis (Fig. 2, *B* and *C*). Conversely, Osx-$Cre^{+/-}Capn4^{+/+}$ mice did not present any detectable bone abnormality at any prenatal or postnatal age. μCT analysis showed no significant differences in 12-week-old male and female Osx-$Cre^{+/-}Capn4^{+/+}$ *versus* $Capn4^{flox/flox}$ when compared with parameters such as bone volume per total volume (16.4 ± 2.0 *versus* 15.3 ± 4.0%), trabecular number (5.1 ± 0.2 *versus* 4.6 ± 0.8/mm), and trabecular spacing (187.3 ± 10.2 *versus* 216.85 ± 44.5 μm) (data for female not shown). These results, thus, exclude any adverse effect of the *Cre* transgene *per se* on bone homeostasis. It is, therefore, likely that lack of a single *Capn4* allele in cells of the osteoblast lineage is sufficient to cause bone loss, which, however, is detectable exclusively in adult mice.

Histomorphometric and μCT analyses were performed on bone specimens of $Capn4^{flox/flox}$ and Osx-$Cre^{+/-}Capn4^{flox/flox}$ mice and confirmed a significant decrease of bone volume and trabecular number with concomitant increase of trabecular spacing in Osx-$Cre^{+/-}Capn4^{flox/flox}$ when compared with $Capn4^{flox/flox}$ control male mice at 12 weeks of age (Fig. 3*A* and data not shown). Moreover, bone formation rate, osteoblast number, and mineral apposition rate were all significantly reduced in Osx-$Cre^{+/-}$ $Capn4^{flox/flox}$ (Fig. 3*A*). Osteoclast number was also significantly decreased in mutants *versus* controls as indicated by both histomorphometry and TRAP staining (Fig. 3*A* and data not shown). Taken together, these data suggest that bone loss observed in Osx-$Cre^{+/-}$ $Capn4^{flox/flox}$ mice is likely the consequence of decreased osteoblast number and activity. Consistent with the findings described above, serum levels of both osteocalcin and TRACP 5b, markers of osteoblast and osteoclast activities, respectively, were markedly reduced in mutant mice (osteocalcin; $Capn4^{flox/flox}$ ($n = 7$), 60.0 ± 5.3 ng/ml; Osx-$Cre^{+/-}Capn4^{flox/flox}$ ($n = 9$), 39.7 ± 2.6* ng/ml. TRACP5b; $Capn4^{flox/flox}$ ($n = 6$), 3.9 ± 0.6 units/liter; Osx-$Cre^{+/-}$ $Capn4^{flox/flox}$ ($n = 10$), 2.7 ± 0.3* units/liter. *, $p < 0.05$).

Lack of Capn4 in Cells of the Osteoblast Lineage Reduces Bone Cortical Thickness and Bone Architecture—Cortical bone morphology was examined by μCT analysis at the mid-femoral diaphysis. Total and cortical bone areas and cortical thickness were significantly reduced in Osx-$Cre^{+/-}Capn4^{flox/flox}$ mice *versus* controls, suggesting that the bone is smaller and that periosteal apposition is inhibited in Osx-$Cre^{+/-}Capn4^{flox/flox}$ mice (Fig. 3*B*). In addition, the polar moment of inertia, an index of torsional strength, was significantly lower in mutants than controls (Fig. 3*B*). Thus, deletion of *Capn4* in cells of the osteoblast lineage causes bone loss in both trabecular and cortical compartments and severely affects parameters that predict bone strength.

Lack of Capn4 Impairs Proliferation of Cells of the Osteoblast Lineage—The reduced osteoblast number observed in Osx-$Cre^{+/-}Capn4^{flox/flox}$ mice could be a consequence of either decreased proliferation or increased apoptosis. To distinguish between these two possibilities, proliferation of cells of the osteoblast lineage was examined by BrdUrd incorporation in 1- and 2-week-old mice. The number of BrdUrd-positive cells detected in the primary spongiosa was significantly reduced in Osx-$Cre^{+/-}Capn4^{flox/flox}$ when compared with Osx-$Cre^{+/-}$ $Capn4^{flox/+}$ and $Capn4^{flox/flox}$ littermates (Fig. 4*B*, *panel 1*), whereas chondrocyte proliferation, which served as an internal control for proper BrdUrd uptake and distribution, was not affected (Fig. 4*B*, *panel 2*). No significant difference in the number of apoptotic cells determined by terminal deoxynucleotidyl transferase-mediated nick-end labeling staining was detected in 2-week-old mutant bones *versus* controls (data not shown). Collectively, these data indicate that the reduced osteoblast

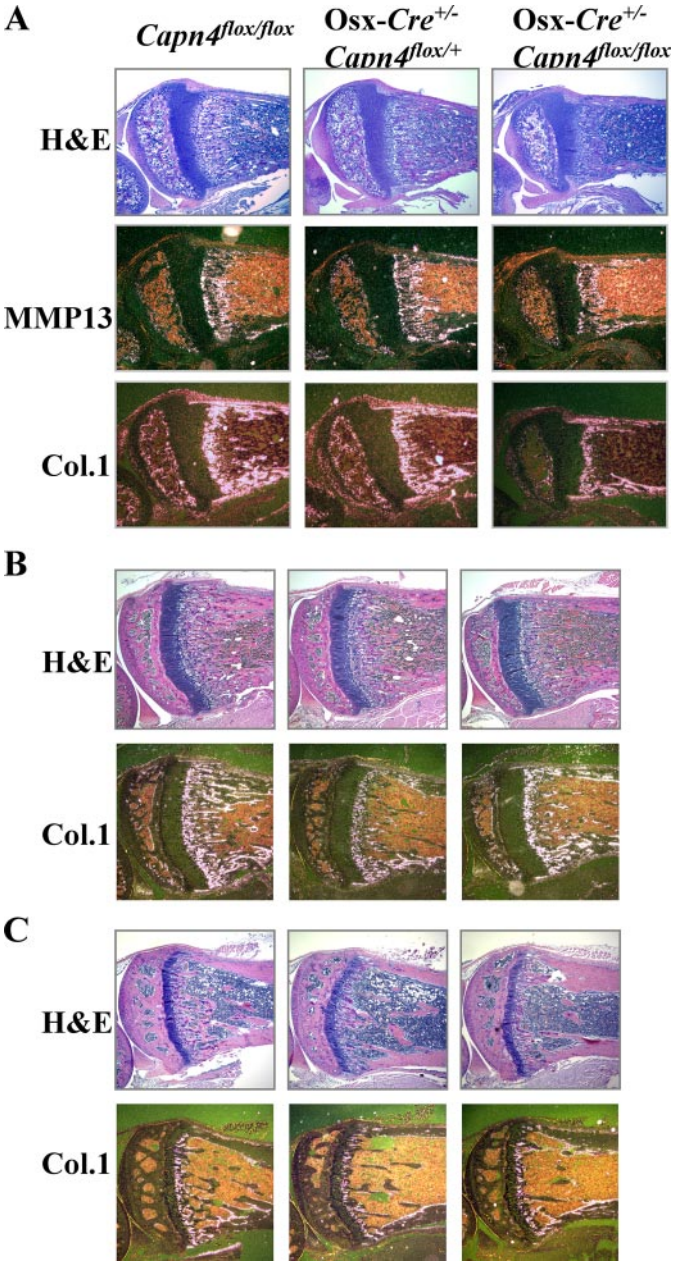

FIGURE 2. **Lack of Capn4 in cells of the osteoblast lineage causes osteoporotic bone phenotype.** *A*, lack of *Capn4* in osteoblasts reduces expression of osteoblast-specific markers in tibias of 2-week-old Osx-$Cre^{+}Capn4^{flox/flox}$ male mice. *H&E*, hematoxylin and eosin. *B* and *C*, lack of *Capn4* in osteoblasts reduces trabecular bone in Osx-$Cre^{+/-}Capn4^{flox/+}$ and Osx-$Cre^{+/-}$-$Capn4^{flox/flox}$ mice *in* 4-week-old (*B*) and 9-week-old males (*C*). *In situ* hybridization was performed using a ribo-probes detecting *Col.1* and *MMP13* mRNA.

number observed in Osx-$Cre^{+/-}Capn4^{flox/flox}$ is likely due to reduced proliferation of cells of the osteoblast lineage.

Lack of Capn4 Impairs Osteoblast Differentiation and Mineralization in Vitro—Osteoblast functions were next investigated *in vitro*. For this purpose, primary calvarial osteoblasts were harvested from Osx-$Cre^{+/-}Capn4^{flox/+}$ and Osx-$Cre^{+/-}Capn4^{flox/flox}$ newborn mice and seeded at a density of 5.0×10^3 cells/cm^2. Levels of *Capn4* mRNA expression were reduced by ~90% in Osx-$Cre^{+/-}Capn4^{flox/flox}$ osteoblasts in comparison with Osx-$Cre^{+/-}Capn4^{flox/+}$. Cell growth was indistinguishable between Osx-$Cre^{+/-}Capn4^{flox/flox}$ and Osx-$Cre^{+/-}Capn4^{flox/+}$ calvarial cells until day 10 and became significantly lower in Osx-$Cre^{+/-}Capn4^{flox/flox}$ cells than Osx-$Cre^{+/-}Capn4^{flox/+}$ cells on day 14. Osteoblast differentiation and mineralization, assessed by ALP activity and mRNA expression of various osteoblast markers, and number of bone nodules, normalized by cell number at the time of assay, respectively, were all significantly lower in Osx-$Cre^{+/-}Capn4^{flox/flox}$ than in Osx-$Cre^{+/-}Capn4^{flox/+}$ calvarial cells (Fig. 5).

Next, to further investigate a role of *Capn4* in osteoblast differentiation, calvarial cells isolated from $Capn4^{flox/flox}$ mice were infected with adenovirus expressing either *Cre*-recombinase (adeno-*Cre*) or β-galactosidase (adeno-*lacZ*). The efficiency of *Cre*-recombinase was assessed at both genomic DNA and RNA levels using real-time qPCR. Approximately 85% of $Capn4^{flox}$ alleles were successfully excised in adeno-*Cre*-infected cells, and their levels of *Capn4* mRNA expression were reduced to less than 10% of those observed in adeno-*lacZ*-infected control cells. Forty-eight h after adenoviral infection, cells were replated at the density of 1.3×10^5 cells/cm^2 (higher density) to allow them to reach an indistinguishable cell number at the time of assay and, thus, minimize the confounding effect of impaired proliferation on the differentiation process. Notably, cell number of both mutant and control cells similarly increased and reached a plateau around day 10, when cells were seeded at the high density (data not shown). When the number of the apoptotic events was determined by annexin V staining, no significant difference was detected in *Capn4*-null calvarial cells when compared with the controls (ratio of annexin V-positive early and late apoptotic cells per total cells; control, 14.3 ± 1.8%; *Capn4*-null, 15.2 ± 1.3%). Consistent with the *in vivo* data, calvarial cells lacking *Capn4* showed significantly reduced ALP activity (Fig. 6*A*) as well as impaired expression of several genes including *NaPi3*, *PGK*, and *Runx2* that are early markers of osteoblast differentiation (Fig. 6*B*) (28). Expression of late markers of osteoblast differentiation such as *ALP*, *Col.1*, and *OC* was also significantly down-regulated in *Capn4*-null cells *versus* controls (Fig. 6*C*). Lastly, *Capn4*-null cells grown in differentiation medium for 21 and 28 days, respectively, formed only 33% of the bone nodules observed in control cells (Fig. 6, *D* and *E*). Taken together, these *in vitro* results confirm that lack of *Capn4* impairs both proliferation and differentiation of cells of the osteoblast lineage as indicated by the *in vivo* model.

Lack of Capn4 in Cells of the Osteoblast Lineage Reduced PTH-stimulated c-fos mRNA Expression in Vitro—To further examine an effect of *Capn4* ablation on gene transcription in cells of the osteoblast lineage, primary calvarial cells were treated with PTH for 0, 1, and 2 h, and levels of c-*fos* mRNA expression were assessed using real-time qPCR. c-*fos* is a key downstream target gene of PTH, and its expression increases rapidly and transiently upon PTH stimulation (31–33). In adeno-*lacZ*-infected control calvarial cells, PTH treatment for 1 and 2 h increased c-*fos* mRNA levels 17- and 9-fold above basal levels, respectively. This effect was reduced by ~35% in adeno-*Cre*-infected *Capn4*-null calvarial cells (Fig. 7*A*). We also silenced the calpain small subunit in UMR cells by using

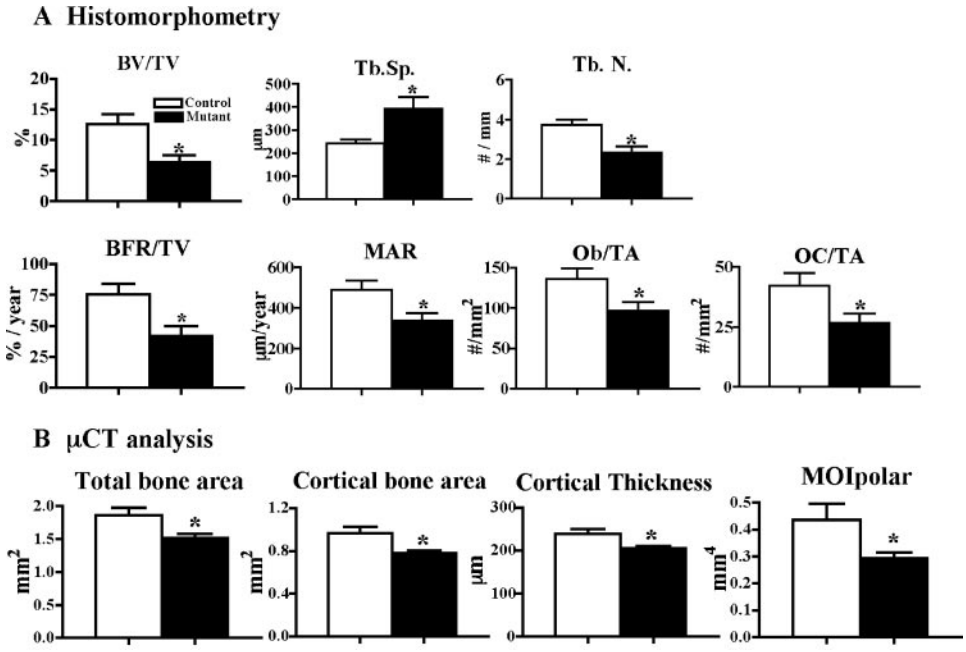

FIGURE 3. **Lack of *Capn4* in osteoblasts causes reduced trabecular bone with thinner cortices in adult mutant mice.** *A*, histomorphometric analysis was performed using tibias of *Capn4*$^{flox/flox}$ control ($n = 6$, *open column*) and Osx-*Cre*$^{+/-}$*Capn4*$^{flox/flox}$ mutant ($n = 6$, *closed column*) male mice. Bone volume per total volume (*BV/TV*); trabecular spacing (*Tb.Sp.*); trabecular number (*Tb.N.*); bone formation rate per total volume (*BFR/TV*); mineral apposition rate (*MAR*); osteoblast number per total area (*Ob/TA*); and osteoclast number per total area (*OC/TA*), as determined by static and dynamic histomorphometry. *B*, lack of *Capn4* in osteoblasts reduces total and cortical bone areas, cortical thickness, and indices of mechanical strength as determined by μCT analysis of the femoral mid-shaft diaphysis. The polar moments of inertia (*MOIpolar*). *Capn4*$^{flox/flox}$ control ($n = 5$, open column) and Osx-*Cre*$^{+/-}$*Capn4*$^{flox/flox}$ mutant ($n = 6$, closed column) male mice. *, $p < 0.05$.

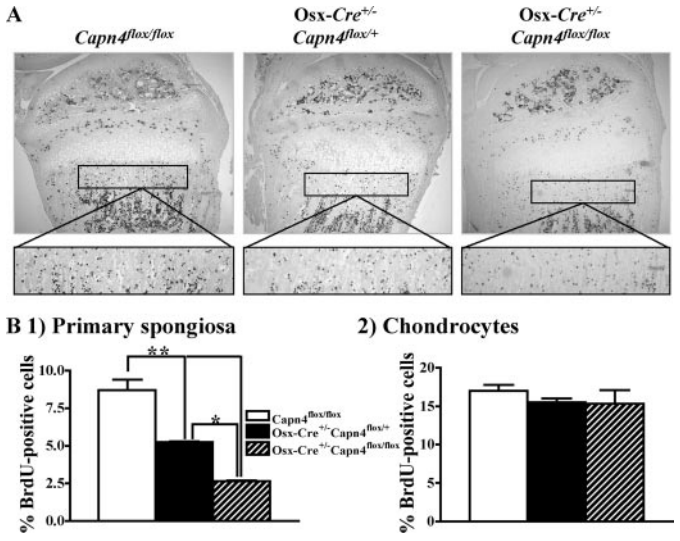

FIGURE 4. **Lack of *Capn4* impairs proliferation of cell of the osteoblast lineage *in vivo*.** *A*, incorporated BrdUrd was detected by immunostaining using anti-BrdUrd antibody in proximal tibias of 2-week-old male mice. *B*, quantitative analysis of BrdUrd (*BrdU*)-positive osteoblasts in primary spongiosa (*panel 1*) and of chondrocytes in the proliferative layer of the growth plate (*panel 2*). *, $p < 0.05$, **, $p < 0.01$.

siRNA technology. siRNAs that specifically targeted *Capn4* (*Capn4*-1 and *Capn4*-2) reduced calpain activity to 25 and 55%, respectively, when compared with control siRNA (Fig. 7*B*, *panel 1*). *Capn4*-knock-out in UMR cells resulted in a significant impairment of PTH-mediated increase of c-*fos* expression (Fig. 7*B*, *panel 2*). Cell surface expression of the receptor for PTH and PTH-related peptide determined by ligand binding assay was indistinguishable between control and *Capn4*-null cells (data not shown). Collectively, these results suggest that *Capn4* could regulate osteoblast function, at least in part, by modulating PTH activity in these cells.

DISCUSSION

Here we report the novel finding that *Capn4* is critically important in bone development and remodeling *in vivo*. Given the early lethality of the universal *Capn4* knock-out embryos, Osx-*Cre*$^{+/-}$*Capn4*$^{flox/flox}$ was an appropriate animal model to investigate the role of the calpain small subunit in cells of the osteoblast lineage (5, 6).

Calpains belong to a family of intracellular cysteine proteases that have been shown to cleave numerous and diverse substrates (1). Our study provided direct evidence that lack of *Capn4* severely affects proliferation of cells of the osteoblast lineage both *in vivo* and *in vitro*. Consistent with these findings, it was previously reported that a cell-permeable calpain inhibitor attenuates proliferation in the MC3T3-E1 cell line (10, 11). The role of calpain in the cell cycle has been controversial. *Capn4*-null embryonic fibroblasts with no calpain activity proliferate normally (5). However, several studies have suggested that calpain plays a role in the cell cycle, mainly at G_1 to S transition, by regulating proteolysis of various proteins such as cyclin D and A, cyclin-dependent kinase 2, and p53 (31–33). Our novel animal model demonstrates that regulation of cell proliferation is indeed a crucial biological function of the calpain small subunit, at least in osteoblasts.

Lack of *Capn4* in osteoblasts significantly reduces ALP activity and expression of differentiation markers such as *ALP*, *Col.1*, *OC*, and *Runx2* mRNAs. Consistent with our findings, a cell-permeable calpain inhibitor was reported to attenuate osteoblast differentiation in the MC3T3-E1 cell line (11). The finding constitutes the first *in vivo* evidence that *Capn4* is an essential modulator of cell terminal differentiation in osteoblasts. Notably, immunostaining for μ- and m-calpains performed in the MC3T3-E1 cell line revealed that m-calpain is a cytoplasmic protein, whereas μ-calpain is both nuclear and cytoplasmic, which implies that calpains may control gene expression directly at the transcriptional level (11).

It has been reported that PTH stimulates expression of the immediate early gene, c-*fos*, which has a critical role in bone biology, by regulating phosphorylation of the cAMP response element binding protein at serine 133 by protein kinase A (34–38). Moreover, we have previously reported that MC3T3-E1 osteoblastic cells stably expressing calpastatin show markedly reduced PTH-mediated cAMP accumulation (2). Lastly, our present study indi-

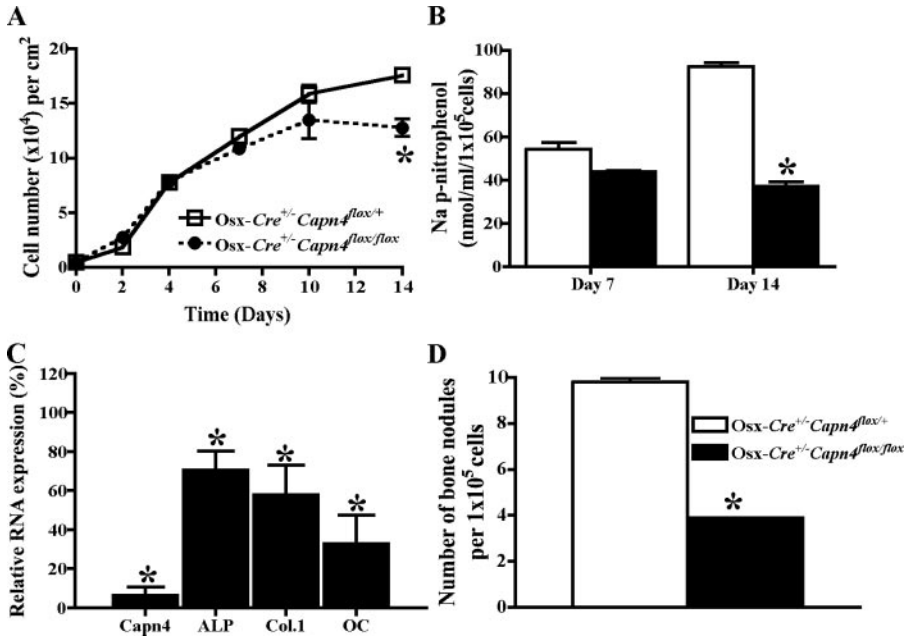

FIGURE 5. **Characterization of primary osteoblasts harvested from Osx-$Cre^{+/-}Capn4^{flox/+}$ and Osx-$Cre^{+/-}Capn4^{flox/flox}$ mice.** *A*, cell number was reduced in Osx-$Cre^{+/-}Capn4^{flox/flox}$ calvarial cells. Cell number was counted on days 0, 2, 5, 7,10, and 14. *B*, ALP activity was lower in Osx-$Cre^{+/-}Capn4^{flox/flox}$ calvarial cells. ALP activity was measured on days 7 and 14 and adjusted by cell number at the time of assay. *C*, expression of markers for osteoblast differentiation was reduced in Osx-$Cre^{+/-}Capn4^{flox/flox}$ calvarial cells. Relative RNA expression of *Capn4*, *ALP*, *Col.1*, and *OC* was determined using real-time qPCR after 7 days in culture. *D*, osteoblast mineralization was reduced in Osx-$Cre^{+/-}Capn4^{flox/flox}$ calvarial cells. Cells were seeded at the density of 5×10^3 cells/cm^2 and cultured in differentiation medium for 21 days. Formation of bone nodules was assessed by Alizarin red S staining. *, $p < 0.05$.

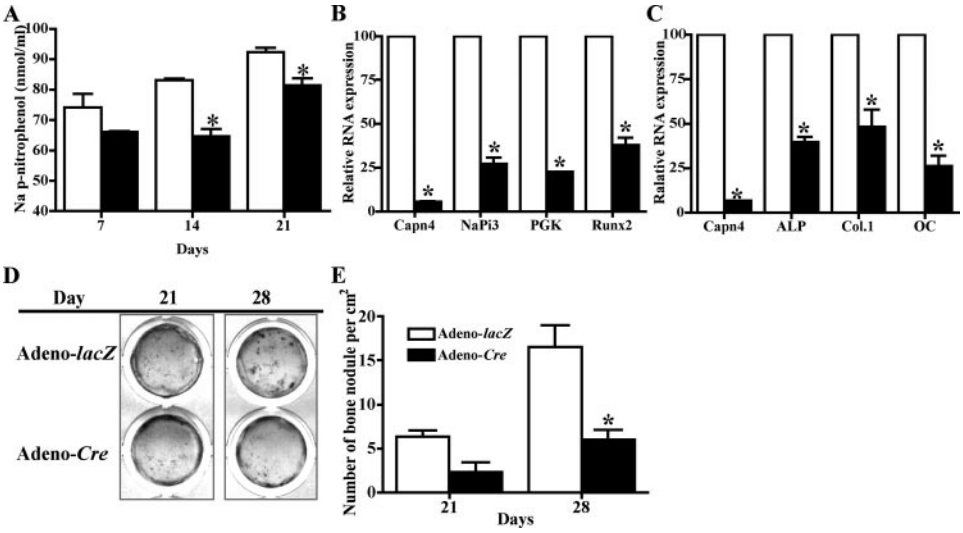

FIGURE 6. **Characterization of primary calvarial cells harvested form $Capn4^{flox/flox}$ mice and infected with adenovirus carrying either *lacZ* or *Cre*.** Cells were infected with either adeno-*LacZ* or adeno-*Cre* and, 48 h later, were replated at the density of 1.3×10^5 cells/cm^2. *A*, lack of *Capn4* in osteoblasts reduced ALP activity in 14- and 21-day culture. *B* and *C*, relative RNA expression of early (*B*; 3-day incubation) and late (*C*; 14-day incubation) markers for osteoblast differentiation was reduced in *Capn4*-null primary calvarial cells. *D* and *E*, lack of *Capn4* in calvarial cells impaired osteoblast mineralization. Images of bone nodules detected by von Kossa staining (*D*) and quantitative analysis of the number of bone nodules (*E*) are shown. *, $p < 0.05$.

cates that lack of *Capn4* reduces PTH-stimulated expression of c-*fos* in both primary calvarial and UMR cells. Collectively, these data thus suggest that *Capn4* may regulate osteoblast functions, at least in part, by modulating PTH activity in these cells.

A role of calpains in bone homeostasis has been previously proposed by the analysis of universal μ-calpain knock-out mice, which develop osteopenia secondary to an increased osteoclast activity. No detectable osteoblast phenotype was reported in these mutant mice (39). Thus, their bone phenotype clearly differs from that of the osteoblast-specific *Capn4* knock-out mice, which showed both impaired osteoblast number and function and reduced osteoclast number and activity. Altogether, the phenotype of the *Capn4* knock-out mice may reflect either loss of m-calpain function or loss of both m-calpains and μ-calpains function in osteoblasts.

Several lines of evidence indicated that lack of a single *Capn4* allele in cells of the osteoblast lineage causes a detectable bone phenotype. Osx-$Cre^{+/-}Capn4^{flox/+}$ mice started to lose body weight around 6 weeks of age, and their mean body weight became indistinguishable from that of Osx-$Cre^{+/-}Capn4^{flox/flox}$ mice at 10 weeks of age. Although body weight only serves as an indirect indicator of skeletal growth, the data suggest impaired skeletal growth in Osx-$Cre^{+/-}Capn4^{flox/+}$ mice. Moreover, histological analysis showed that Osx-$Cre^{+/-}Capn4^{flox/+}$ mice rapidly develop an osteoporotic phenotype between 2 and 4 weeks of age. Lastly, proliferation of cells of the osteoblast lineage as assessed by BrdUrd incorporation at 2 weeks was significantly reduced in Osx-$Cre^{+/-}Capn4^{flox/+}$ mice when compared with $Capn4^{flox/flox}$ mice, although it was still ~2-fold higher than in Osx-$Cre^{+/-}Capn4^{flox/flox}$ specimens. Importantly, Osx-$Cre^{+/-}Capn4^{+/+}$ were, virtually and as confirmed by μCT analysis, indistinguishable from wild-type controls, which indicates that the bone phenotype of Osx-$Cre^{+/-}Capn4^{flox/+}$ was not the mere consequence of a nonspecific effect secondary to the presence of the *Cre* transgene in cells of the osteoblast lineage. These results are suggestive of a possible haploinsufficiency phenotype in mice lacking one allele of *Capn4* in cells of the osteoblast lineage.

In summary, lack of *Capn4* in cell of the osteoblast lineage negatively affects both trabecular and cortical bone by impairing proliferation and differentiation of osteoblastic cells. Our

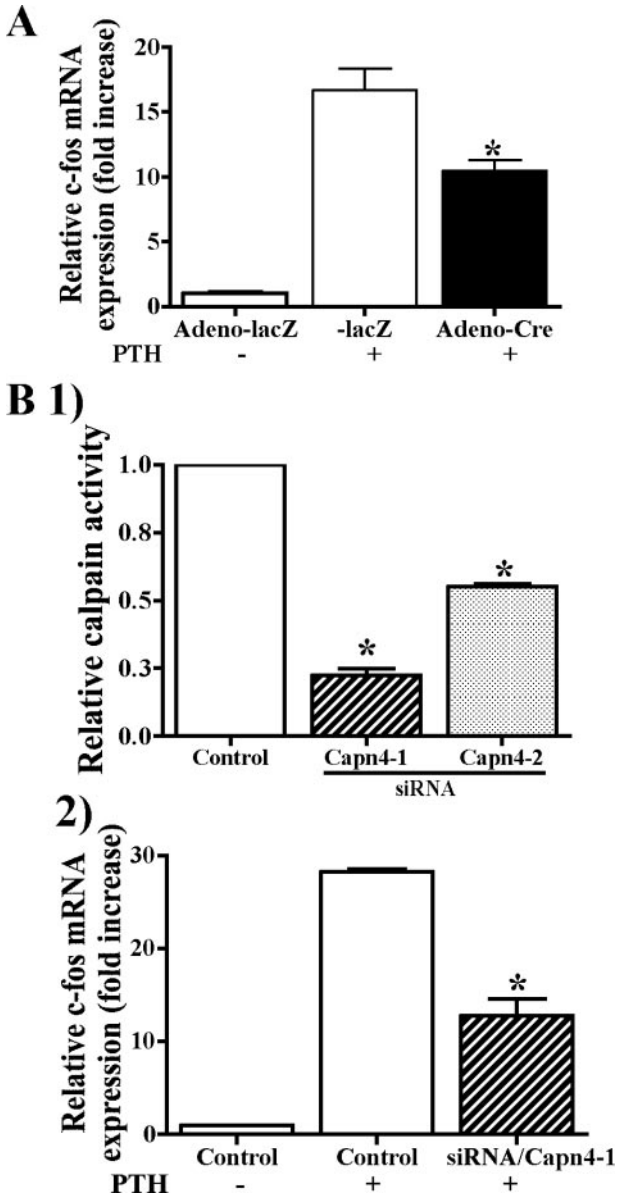

FIGURE 7. **Lack of *Capn4* reduced PTH-stimulated c-*fos* mRNA expression in cells of the osteoblast lineage.** *A*, primary calvarial cells harvested from *Capn4*$^{flox/flox}$ mice were infected with either adeno-*lacZ* or -*Cre*. Forty-eight h later, cells were stimulated with 1×10^{-7} M PTH for 1 h, and c-*fos* mRNA expression was quantified using real-time qPCR. The mean value of c-*fos* expression before PTH stimulation in control cells was set as 1. *B*, *panel 1*, efficiency of *Capn4* siRNA in silencing *Capn4* was assessed by calpain activity. UMR cells were transfected with siRNAs that specifically targeted *Capn4* (*Capn4*-1 and *Capn4*-2) for 24 h and incubated in fresh medium for additional 24 h. Calpain activity was reduced to 25 and 55% in UMR cells transfected with siRNA/*Capn4*-1 and -2, respectively. *Panel 2*, control and *Capn4*-null (siRNA/*Capn4*-1) calvarial cells were treated with 1×10^{-7} M PTH for 1 h, and c-*fos* mRNA expression was quantified using real-time qPCR. *, $p < 0.05$.

data thus indicate that calpains could be important molecules in pathological conditions such as osteoporosis.

Acknowledgments—We thank Dr. Henry M. Kronenberg for critical review of the manuscript and helpful discussion. We also thank Clare Thomas, Kimberly Atkin, Cornelia Withington, Dilani Rossa, and Yuko Sumiyama at MGH, and David Panus at Beth Israel Deaconess Medical Center for technical supports.

REFERENCES

1. Goll, D. E., Thompson, V. F., Li, H., Wei, W., and Cong, J. (2003) *Physiol. Rev.* **83,** 731–801
2. Shimada, M., Mahon, M. J., Greer, P. A., and Segre, G. V. (2005) *Endocrinology* **146,** 2336–2344
3. Sternberg, N., and Hamilton, D. (1981) *J. Mol. Biol.* **150,** 467–486
4. Cong, J., Goll, D. E., Peterson, A. M., and Kapprell, H. P. (1989) *J. Biol. Chem.* **264,** 10096–10103
5. Arthur, J. S., Elce, J. S., Hegadorn, C., Williams, K., and Greer, P. A. (2000) *Mol. Cell Biol.* **20,** 4474–4481
6. Zimmerman, U. J., Boring, L., Pak, J. H., Mukerjee, N., and Wang, K. K. (2000) *IUBMB Life* **50,** 63–68
7. Tram, K. K., Spencer, M. J., Murray, S. S., Lee, D. B., Tidball, J. G., and Murray, E. J. (1993) *Biochem. Mol. Biol. Int.* **29,** 981–987
8. Tram, K. K., Murray, S. S., Lee, D. B., and Murray, E. J. (1993) *Kidney Int.* **43,** 693–699
9. Murray, E. J., Murray, S. S., Tram, K. K., and Lee, D. B. (1994) *Exp. Cell Res.* **215,** 241–248
10. Murray, E. J., Grisanti, M. S., Bentley, G. V., and Murray, S. S. (1997) *Metab. Clin. Exp.* **46,** 1090–1094
11. Murray, S. S., Grisanti, M. S., Bentley, G. V., Kahn, A. J., Urist, M. R., and Murray, E. J. (1997) *Exp. Cell Res.* **233,** 297–309
12. Reeve, J., Hesp, R., Williams, D., Hulme, P., Klenerman, L., Zanelli, J. M., Darby, A. J., Tregear, G. W., and Parsons, J. A. (1976) *Lancet* **1,** 1035–1038
13. Kronenberg, H. M., Lanske, B., Kovacs, C. S., Chung, U. I., Lee, K., Segre, G. V., Schipani, E., and Juppner, H. (1998) *Recent Prog. Horm. Res.* **53,** 283–303
14. Schipani, E., and Provot, S. (2003) *Birth Defects Res. Part C. Embryo Today Rev.* **69,** 352–362
15. Tan, Y., Dourdin, N., Wu, C., De Veyra, T., Elce, J. S., and Greer, P. A. (2006) *Genes. J. Genet. Dev.* **44,** 297–303
16. Nakashima, K., Zhou, X., Kunkel, G., Zhang, Z., Deng, J. M., Behringer, R. R., and de Crombrugghe, B. (2002) *Cell* **108,** 17–29
17. Rodda, S. J., and McMahon, A. P. (2006) *Development* (*Camb.*) **133,** 3231–3244
18. Shimada, M., Shimano, H., Gotoda, T., Yamamoto, K., Kawamura, M., Inaba, T., Yazaki, Y., and Yamada, N. (1993) *J. Biol. Chem.* **268,** 17924–17929
19. Arthur, J. S., Greer, P. A., and Elce, J. S. (1998) *Biochim. Biophys. Acta* **1388,** 247–252
20. McLeod, M. J. (1980) *Teratology* **22,** 299–301
21. Calvi, L. M., Sims, N. A., Hunzelman, J. L., Knight, M. C., Giovannetti, A., Saxton, J. M., Kronenberg, H. M., Baron, R., and Schipani, E. (2001) *J. Clin. Investig.* **107,** 277–286
22. Lee, K., Lanske, B., Karaplis, A. C., Deeds, J. D., Kohno, H., Nissenson, R. A., Kronenberg, H. M., and Segre, G. V. (1996) *Endocrinology* **137,** 5109–5118
23. Bouxsein, M. L., Pierroz, D. D., Glatt, V., Goddard, D. S., Cavat, F., Rizzoli, R., and Ferrari, S. L. (2005) *J. Bone Miner. Res.* **20,** 635–643
24. Bouxsein, M. L., Myers, K. S., Shultz, K. L., Donahue, L. R., Rosen, C. J., and Beamer, W. G. (2005) *J. Bone Miner. Res.* **20,** 1085–1092
25. Glatt, V., Canalis, E., Stadmeyer, L., and Bouxsein, M. L. (2007) *J. Bone Miner. Res.* **22,** 1197–1207
26. Pfander, D., Kobayashi, T., Knight, M. C., Zelzer, E., Chan, D. A., Olsen, B. R., Giaccia, A. J., Johnson, R. S., Haase, V. H., and Schipani, E. (2004) *Development* (*Camb.*) **131,** 2497–2508
27. Gori, F., Divieti, P., and Demay, M. B. (2001) *J. Biol. Chem.* **276,** 46515–46522
28. Liu, X., Bruxvoort, K. J., Zylstra, C. R., Liu, J., Cichowski, R., Faugere, M. C., Bouxsein, M. L., Wan, C., Williams, B. O., and Clemens, T. L. (2007) *Proc. Natl. Acad. Sci. U. S. A.* **104,** 2259–2264
29. Ahdjoudj, S., Kaabeche, K., Holy, X., Fromigue, O., Modrowski, D., Zerath, E., and Marie, P. J. (2005) *Exp. Cell Res.* **303,** 138–147
30. Okahashi, N., Inaba, H., Nakagawa, I., Yamamura, T., Kuboniwa, M., Nakayama, K., Hamada, S., and Amano, A. (2004) *Infect Immun.* **72,** 1706–1714
31. Choi, Y. H., Lee, S. J., Nguyen, P., Jang, J. S., Lee, J., Wu, M. L., Takano, E.,

Maki, M., Henkart, P. A., and Trepel, J. B. (1997) *J. Biol. Chem.* **272,** 28479–28484
32. Carragher, N. O., Westhoff, M. A., Riley, D., Potter, D. A., Dutt, P., Elce, J. S., Greer, P. A., and Frame, M. C. (2002) *Mol. Cell Biol.* **22,** 257–269
33. Zhang, W., Lu, Q., Xie, Z. J., and Mellgren, R. L. (1997) *Oncogene* **14,** 255–263
34. Caubet, J. F., and Bernaudin, J. F. (1988) *Biol. Cell* **64,** 101–104
35. Lee, K., Deeds, J. D., Chiba, S., Un-No, M., Bond, A. T., and Segre, G. V. (1994) *Endocrinology* **134,** 441–450
36. Demiralp, B., Chen, H. L., Koh, A. J., Keller, E. T., and McCauley, L. K. (2002) *Endocrinology* **143,** 4038–4047
37. Pearman, A. T., Chou, W. Y., Bergman, K. D., Pulumati, M. R., and Partridge, N. C. (1996) *J. Biol. Chem.* **271,** 25715–25721
38. Tyson, D. R., Swarthout, J. T., and Partridge, N. C. (1999) *Endocrinology* **140,** 1255–1261
39. Marzia, M., Chiusaroli, R., Neff, L., Kim, N. Y., Chishti, A. H., Baron, R., and Horne, W. C. (2006) *J. Biol. Chem.* **281,** 9745–9754